JOURNAL OF MATERIALS SCIENCE 30 (1995) 2640–2647

Effect of Nb coating on the sulphidation/oxidation behaviour of Ti and Ti–6Al–4V alloy

H.L. DU, P. K. DATTA, J. S. BURNELL-GRAY
Surface Engineering Research Group, University of Northumbria at Newcastle, Newcastle upon Tyne, UK

D. B. LEWIS
Materials Research Institute, Sheffield Hallam University, Sheffield, UK

The environmental response of Nb-coated Ti and Ti–6Al–4V alloy was studied at 750 °C in an atmosphere of $pS_2 \sim 10^{-1}$ Pa and $pO_2 \sim 10^{-18}$ Pa. By acting as a diffusion barrier and through the formation of a $Nb_{1-x}S$ scale the Nb coating deposited enhanced the corrosion resistance of both Ti and Ti–6Al–4V alloy. The corrosion products generated on uncoated titanium in the same environment and temperature were characterized by a double layered oxide scale of TiO_2 beneath which a TiS_2 layer was formed. For the Ti–6Al–4V alloy, α-Al_2O_3 was precipitated in the external portion of the outer-layer of TiO_2 whilst a layer containing Al_2S_3, TiS_2 and vanadium sulphide (possibly V_2S_3) was idenitified underlying the inner TiO_2 layer. After prolonged exposure (168 h), the Nb coating deposited on Ti and Ti–6Al–4V alloy was consumed. A scale following the sequence of $TiO_2/TiO_2+NbO_2+Nb_2O_5/Nb_{1-x}S/TiO_2/TiS_2$/(substrate) was observed on the surface of the Nb-coated Ti, whilst a scale with sequence of $TiO_2/V_2S_3/TiO_2+NbO_2+Nb_2O_5/Nb_{1-x}S/TiO_2/Al_2S_3+TiS_2$/(substrate) characterized the corrosion products formed on the Nb-coated Ti–6Al–4V alloy.

1. Introduction

Ti and Ti-alloys are widely used in the aero-industries and in demanding high temperature applications. However, the environmental degradation of Ti and Ti-alloys at elevated temperatures poses a major technological problem threatening to limit the exploitation of these materials [1–3]. Ti is potentially a highly reactive metal capable of forming thermodynamically stable oxides, nitrides, carbides and sulphides when exposed to oxygen, air, carbonaceous and sulphur-containing gases. Of particular significance is its ability also to dissolve large quantities of gaseous species, a process accompanied by severe embrittlement. More recently, Du and Datta *et al.* [4, 5] investigated the high temperature corrosion behaviour of Ti and Ti–6Al–4V alloys at 750 °C in air, H_2/H_2O and $H_2/H_2O/H_2S$ environments and recorded rapid degradation rates and complex scaling patterns.

Much research has been devoted to developing oxidation resistant Ti alloys. Additions of Cr, e.g. at 5 or 10 wt% level have been observed to increase the observed weight gains, although interestingly both these alloys exhibited reduced scale thickness, the overall increase in weight being associated with greater amounts of dissolved oxygen [6]. Such an effect is related to the microstructure of the Ti–Cr alloys, Cr being a β-stabilizing element [7]. However, it has been reported that at high Cr concentrations (> 10 wt%), Cr has a beneficial effect on the oxidation resistance of titanium, particularly at low temperatures [8]. It is well established that additions of Al to conventional Fe, Ni and Co-based alloys produce a stable and protective α-Al_2O_3 scale. However, in Ti–Al alloys, Ti and Al form oxides of very similar stability [9, 10], but only Al forms a slowly growing oxide (Al_2O_3), whilst all Ti oxides have relatively high growth rates [11]. As a result, even TiAl with ~ 50 at% Al does not form a protective Al_2O_3 scale [12]. Datta [13] pointed out that although the new high temperature titanium alloys – IMI829 and IMI834 – have been developed with temperature capabilities up to 650 °C, they lack the microstructural and thermal stability required to withstand exposure at this temperature for long durations. There is, therefore, a need to address the question of how to protect such alloys against environmental degradation at elevated temperatures and in complex environments.

A significant amount of work has been carried out at Newcastle [14–18] and other laboratories [19–24] towards developing alloys/coatings capable of resisting high temperature degradation in sulphur/oxygen environments. It has been found that several Group IV–VI metals (i.e. V, Nb, Ta, Mo and W) which form sulphides with high melting points, implying low ionic diffusion rates, suffer low or very low rates of degradation in $H_2/H_2O/H_2S$ atmospheres at elevated

0022–2461

temperature. Particularly, the sulphidation rate of Nb is similar to the oxidation rate of Cr ($K_p \sim 10^{-13}$ $g^2 cm^{-4} s^{-1}$) [16]. Also, some progress has been made by the Newcastle Research Group in understanding the scaling behaviour of CoCrAlYX-type alloys, where X is V, Nb, Mo and W at 5–10 wt % levels, after isothermal exposure at 750 °C to a predominantly sulphidizing environment ($pS_2 \sim 10^{-1}$ Pa and $pO_2 \sim 10^{-18}$ Pa) for exposure periods of up to 240 h. Here analysis of the kinetic data and morphological features indicated that such alloys had superior sulphidation resistance relative to that of the CoCrAlY-based alloy without "X" additions [17, 18].

In the present research programme, the effects of a Nb coating laid down by physical vapour deposition (PVD) on the sulphidation/oxidation behaviour of Ti and Ti–6Al–4V alloy were studied at 750 °C in an atmosphere of $H_2/H_2O/H_2S$ ($pS_2 \sim 10^{-1}$ Pa and $pO_2 \sim 10^{-18}$ Pa).

2. Experimental procedure

The commercial substrate materials Ti and Ti–6Al–4V (IMI Titanium 318) were supplied in rod form. The specimens were machined from rods into coupons having sizes of 12.5 mm diameter with 1.5 mm thickness. A 1-mm diameter hole was drilled near the edge of the samples to facilitate easy suspension. Prior to coating deposition all coupons were polished using SiC paper up to 1200 grit followed by ultrasonic cleaning and degreasing in acetone for 30 min. The required Nb coating was deposited in a PVD arc evaporation unit (Multi-Arc), where a vacuum arc was employed for the generation of both the coating flux and ionization necessary for the deposition [25, 26]. The deposition parameters for Nb coating on Ti and Ti–6Al–4V alloy are given in Table I. Following deposition the Nb-coated and uncoated specimens were ultrasonically cleaned again in acetone for 30 min in order to remove any dirt and grease caused during the handling process.

The sulphidation/oxidation kinetics of the Nb-coated and uncoated Ti and Ti–6Al–4V alloy specimens were recorded by using a discontinuous gravimetric method after exposure to a pre-mixed $H_2/H_2O/H_2S$ gas mixture which was designed to yield an atmosphere of ($pS_2 \sim 10^{-1}$ Pa and $pO_2 \sim 10^{-18}$ Pa) at the reaction temperature 750 °C. Details of the experimental rig have been already reported [18, 27–29]. The corrosion products generated on both Nb-coated and uncoated specimens were characterized by scanning electron microscopy (SEM), energy dispersive X-ray analysis (EDX) and X-ray diffraction (XRD). EDX quantitative analysis was performed at an accelerating voltage (20 kV) using a spot size of 100 nm. The results were quantified using a ZAF FL8 routine and oxygen results were determined by difference. The presence of various phases in the multi-layered scales developed on both coated and uncoated Ti and Ti–6Al–4V alloy after various exposures was identified by XRD analysis following sequential removal of layers using a series of polishing operations starting from the surface.

3. Experimental results

3.1. Corrosion kinetics

Weight gain data plotted against exposure time are given in Fig. 1 for the exposed Nb-coated and uncoated titanium and Ti–6Al–4V alloy after sulphidation/oxidation at 750 °C for up to 240 h. It is apparent that the sulphidation/oxidation of Ti followed a linear rate law with a linear rate constant of 5.7×10^{-8} $g cm^{-2} s^{-1}$, whilst that of Ti–6Al–4V alloy obeyed a quasi-parabolic kinetic (the reaction index ~ 1.5) with the corrosion rate decreasing with lengthening exposure time. Parabolic kinetics were observed for the Nb-coated Ti up to 72 h exposure with $K_p \sim 3.4 \times 10^{-11}$ $g^2 cm^{-4} s^{-1}$ and subsequently its behaviour slightly deviated from the parabolic pattern, which reflected a reduced protectiveness of the Nb coating. The enhancement of sulphidation/oxidation resistance of Ti–6Al–4V alloy by the use of Nb coating was significant throughout the whole exposure period (240 h) and a parabolic rate constant of $K_p \sim 2.4 \times 10^{-11}$ $g^2 cm^{-4} s^{-1}$ was calculated.

From the foregoing kinetics data, it can be concluded that the Nb coating used greatly increased

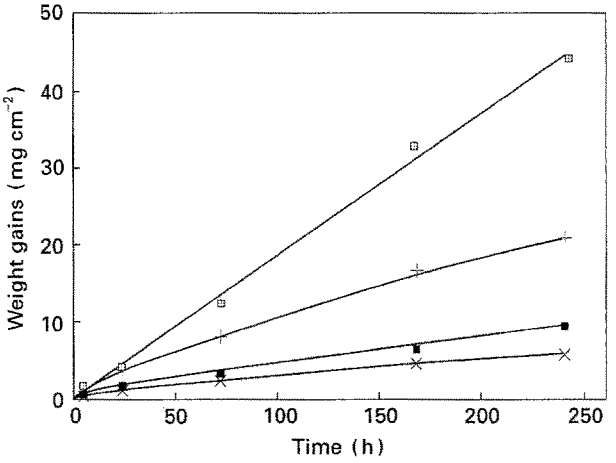

Figure 1 Weight gains against exposure time for Nb-coated and uncoated Ti and Ti–6Al–4V alloy exposed in an $H_2/H_2O/H_2S$ ($pS_2 \sim 10^{-1}$ Pa and $pO_2 \sim 10^{-18}$ Pa) environment at 750 °C. (▨) Ti; (+)Ti–6Al–4V; (■) Ti + Nb; (×)Ti–6Al–4V + Nb.

TABLE I Deposition parameters for Nb coating on Ti and Ti-6A1-4V alloy

Cathode material	Voltage (V)	No. of evaporators	Amp (A)	Amphour (A h)	Ar gas pressure (Pa)	Coating thickness (μm)
Nb	50	2	50	75	2	6

the sulphidation/oxidation resistance of Ti and Ti–6Al–4V alloy in such an aggressive atmosphere.

3.2. Corrosion products

3.2.1. Uncoated Ti and Ti–6Al–4V alloy

After Ti and Ti–6Al–4V alloy were exposed to the test environment ($pS_2 \sim 10^{-1}$ Pa and $pO_2 \sim 10^{-18}$ Pa) at 750 °C, the corrosion products formed consisted basically of three subscale layers which are illustrated in Figs 2 and 3 respectively. For Ti, both the outer-layer and the mid-layer comprised TiO_2 (rutile) which was confirmed by XRD and no compositional nor structural differences were distinguishable between these two subscale layers. It is believed that the outer-layer was formed by the outward diffusion of titanium whilst the mid-layer was produced by the inward diffusion of oxygen. An inner-layer of TiS_2 was found to exist beneath the rutile scale. Also, a copious amount of titanium hydride in acicular pattern, identified as TiH_2 by XRD, was observed in the substrate, as shown by the micrograph in Fig. 2. Obviously, when Ti was exposed to the hydrogen-dominant $H_2/H_2O/H_2S$ environment at the test temperature, hydrogen became readily soluble in the substrate and precipitated as a needle-like hydride.

In the case of Ti–6Al–4V alloy, Al enrichment was evident in the external portion of the outer-layer, i.e. a mixture of Al_2O_3 and TiO_2 was generated. However, a pure TiO_2 layer formed beneath this mixed layer. A mixture of sulphides of Al, Ti and V was recognized between the oxide scale and substrate – here Al_2S_3 and TiS_2 were identified. Significantly, vanadium oxide was found at the interface between the outer and inner TiO_2 layers. Clearly, some vanadium which had diffused outward gathered at this interface (Fig. 3). However it was difficult to identify the presence of vanadium sulphide by XRD, owing perhaps to the small volume fraction present. No titanium hydride in the substrate was evident in this alloy even after 240 h exposure.

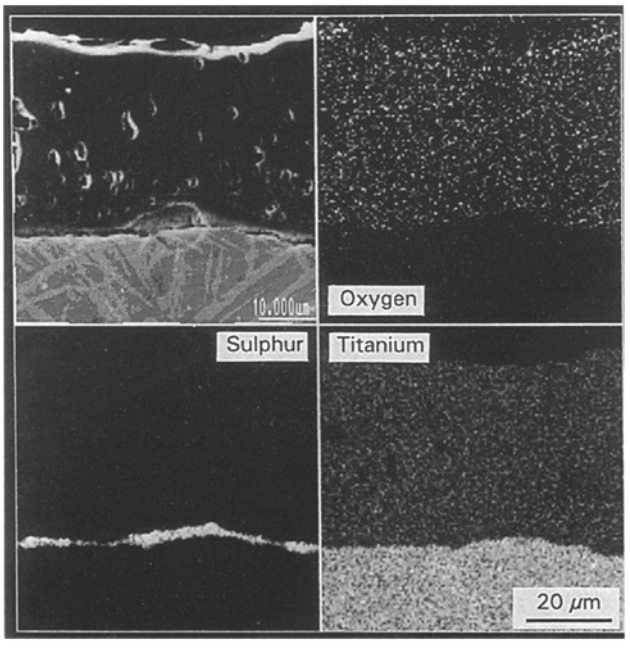

Figure 2 Electron image and Digimaps showing typical morphological and compositional profiles through the scale on Ti after 72 h exposure in an $H_2/H_2O/H_2S$ ($pS_2 \sim 10^{-1}$ Pa and $pO_2 \sim 10^{-18}$ Pa) environment at 750 °C.

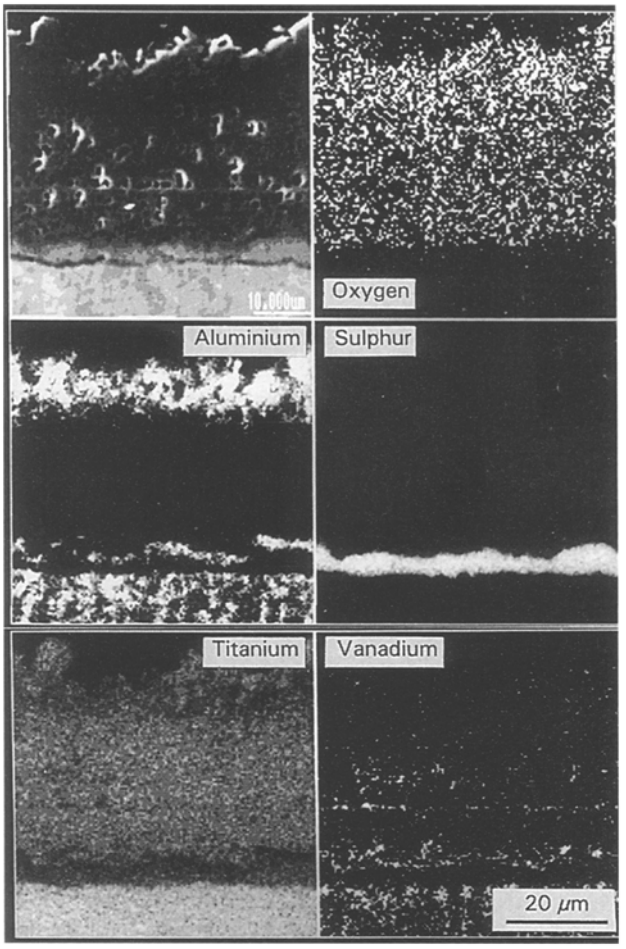

Figure 3 Electron image and Digimaps showing typical morphological and compositional profiles through the scale on Ti–6Al–4V alloy after 72 h exposure in an $H_2/H_2O/H_2S$ ($pS_2 \sim 10^{-1}$ Pa and $pO_2 \sim 10^{-18}$ Pa) environment at 750 °C.

3.2.2. Nb-coated Ti and Ti–6Al–4V alloy

The Nb coating deposited modified the corrosion mechanism controlling the process of sulphidation/oxidation of Ti and Ti–6Al–4V alloy in the environment ($pS_2 \sim 10^{-1}$ Pa and $pO_2 \sim 10^{-18}$ Pa) at 750 °C. Fig. 4 shows line scanning compositional profiles through the scale formed on the Nb coated Ti after 5 h sulphidation/oxidation. It was found by XRD analysis (not shown here) that $Nb_{1-x}S$ scale was formed on the top of Nb coating and then Ti diffused outward and produced TiO_2 on the $Nb_{1-x}S$ scale. From Fig. 5 it can be noted that the TiO_2 layer did not completely cover the previously formed $Nb_{1-x}S$ scale. XRD analysis indicated that a large amount of Nb coating was still present on the substrate. Fig. 4 further indicates that sulphur species diffused through the Nb coating and reacted with Ti to form TiS_2. The presence of TiS_2 was also confirmed by XRD.

Fig. 6 shows a scanning electron micrograph of the Nb coated Ti after 240 h sulphidation/oxidation. The

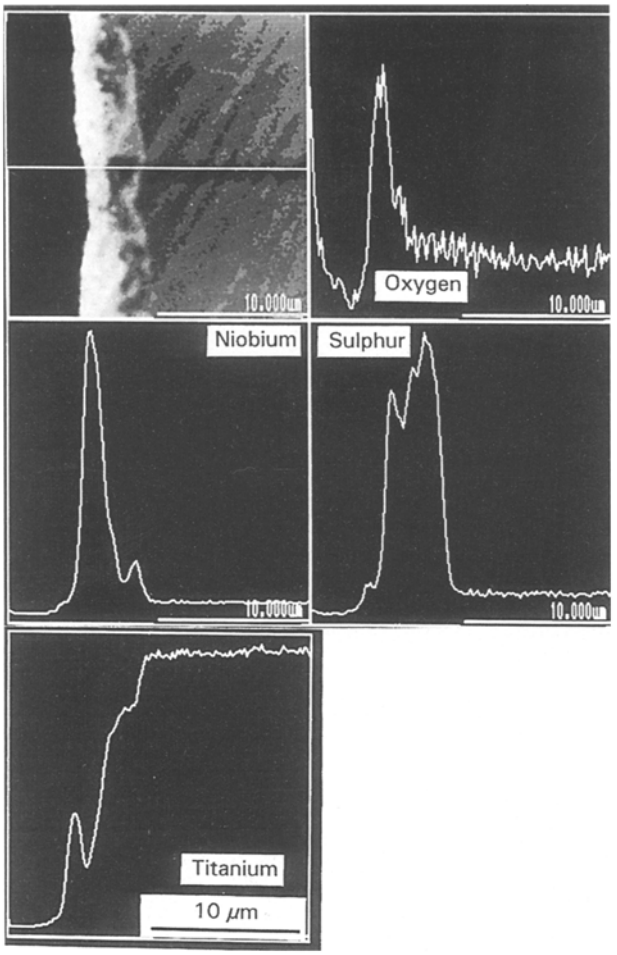

Figure 4 Electron morphological image and compositional profiles through the scale on Nb-coated Ti after 5 h exposure in an $H_2/H_2O/H_2S$ ($pS_2 \sim 10^{-1}$ Pa and $pO_2 \sim 10^{-18}$ Pa) environment at 750 °C.

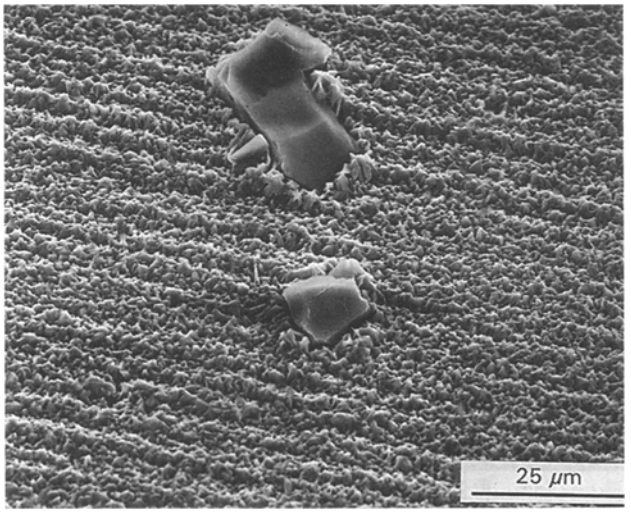

Figure 5 Scanning electron micrograph showing typical surface morphology of Nb-coated Ti after 5 h exposure in an $H_2/H_2O/H_2S$ ($pS_2 \sim 10^{-1}$ Pa and $pO_2 \sim 10^{-18}$ Pa) enviroment at 750 °C.

quantitative EDX results at different locations (marked A, B, C, D, E and F in Fig. 6) through the scale are listed in Table II. Error values quoted in Table II are the standard deviation of the analysis of individual elements. The XRD profiles for the Nb-coated Ti after 168 h exposure are depicted in Fig. 7. Trace 1 represents the surface of XRD without any polishing whilst trace 2 reveals the XRD results obtained after a series of polishing which removed most of the outer TiO_2 layer. The corresponding phases identified are given in Table III. Combining the EDX (Fig. 6) and XRD (Fig. 7) results it can be said that in the outermost area (point A), a TiO_2 layer was formed beneath which (point B) a mixture of TiO_2 and $NbO_2 + Nb_2O_5$ developed. At the interface of the outer TiO_2 layer and $TiO_2 + NbO_2 + Nb_2O_5$ mixed layer, some voids are observed which occurred at the TiO_2 side. At point C, a layer of mainly $Nb_{1-x}S$ (also containing some TiO_2) developed. The innermost layer (Point E) consisted mainly of TiS_2 with a small amount of TiO_2. Interestingly a TiO_2 layer was also formed between the $Nb_{1-x}S$ and TiS_2 layer (Point D). At Point F, 99%Ti was recorded.

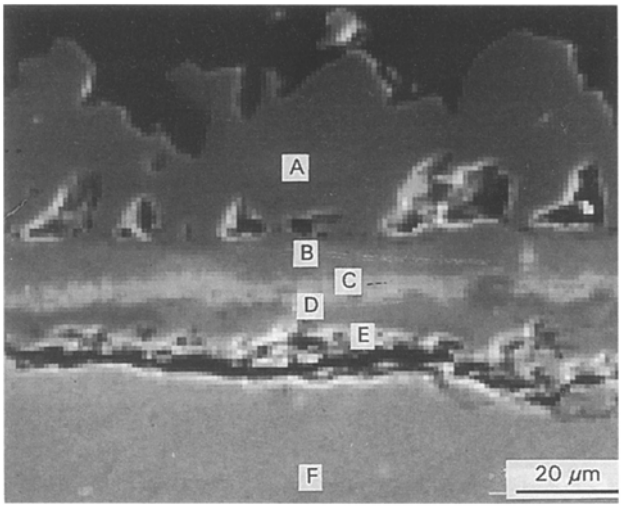

Figure 6 Scanning electron micrograph showing typical cross-sectioned scale on Nb-coated Ti after 240 h exposure in an $H_2/H_2O/H_2S$ ($pS_2 \sim 10^{-1}$ Pa and $pO_2 \sim 10^{-18}$ Pa) environment at 750 °C.

A more complicated picture was revealed for the Nb-coated Ti–6Al–4V alloy with respect to Nb-coated Ti. Fig. 8 contains a SEM micrograph and the Digimaps typical of the Nb-coated Ti–6Al–4V alloy after 240 h exposure. The XRD patterns for the 168 h exposed sample are also illustrated in Fig. 9 in which traces 1 and 2 represent XRD results without and with polishing respectively. Like the Nb-coated Ti, the outermost layer comprised TiO_2 underlying which a $TiO_2 + NbO_2 + Nb_2O_5$ mixed layer developed. There was no evidence for the presence of Al_2O_3 in this layer as was observed for the uncoated Ti–6Al–4V. However, a discontinuous layer of vanadium sulphide (V_2S_3 confirmed by quantitative EDX data) was present between the outermost TiO_2 layer and the mixed layer of $TiO_2 + NbO_2 + Nb_2O_5$. In addition some voids were formed at the TiO_2 side. The next layer consisted of $Nb_{1-x}S$ below which another TiO_2 layer was identified. The innermost layer consisted of Al_2S_3 and TiS_2.

It should be pointed out that there was little evidence to demonstrate the existence of Nb coating after 168 h sulphidation/oxidation and the Nb coating was found to be completely consumed.

TABLE II The quantitative EDX results for the Nb-coated Ti after 240 h exposure

Point	Elemental composition (wt%) Ti	Error (%)	Nb	Error (%)	S	Error (%)	O	Phase present
A	61.75	0.22	–		–		38.25[a]	TiO_2
B	44.8	0.2	19.13	0.19	–		35.68[a]	TiO_2, NbO_2, Nb_2O_5
C	18.28	0.14	49.63	0.31	22.15	0.14	9.94[a]	$Nb_{1-x}S$, (TiO_2)
D	53.89	0.21	6.93	0.2	9.43	0.13	29.76[a]	TiO_2, ($Nb_{1-x}S$)
E	60.25	0.22	–		24.85	0.12	13.68[a]	TiS_2, (TiO_2)
F	99.9	0.23	–		–		–	Ti

Note ( ) represent uncertain phases.
[a] Oxygen contents were determined by difference.

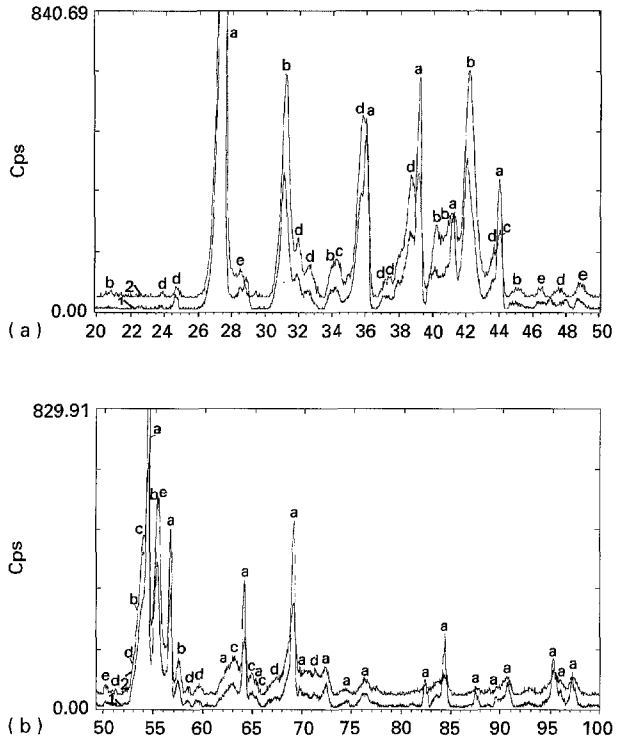

Figure 7 XRD profiles of Nb-coated Ti after 168 h exposure in an $H_2/H_2O/H_2S$ ($pS_2 \sim 10^{-1}$ Pa and $pO_2 \sim 10^{-18}$ Pa) environment at 750 °C. (a) Theta = 20–50 degree; (b) Theta = 50–100 degree.

TABLE III Phases detected and JCPDS numbers

Marks	Phase	JCPDS number
a	TiO_2	21-1276
b	$Nb_{1-x}S$	22-1200
c	TiS_2	15-0835
d	NbO_2	19-0859
e	Nb_2O_5	28-0317
f	Al_2S_3	24-0014
g	Ti	5-0682

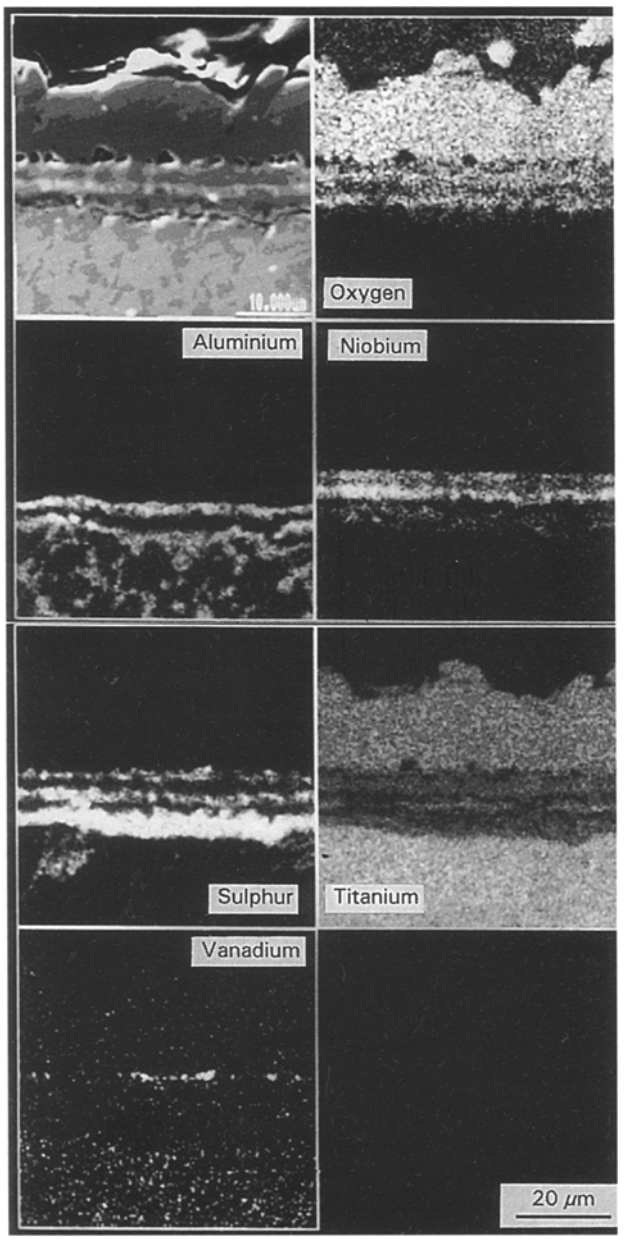

Figure 8 Electron image and Digimaps showing typical morphological and compositional profiles through the scale on Nb-coated Ti–6Al–4V alloy after 240 h exposure in an $H_2/H_2O/H_2S$ ($pS_2 \sim 10^{-1}$ Pa and $pO_2 \sim 10^{-18}$ Pa) environment at 750 °C.

4. Discussion

The Nb coating deposited on Ti and Ti–6Al–4V alloy, firstly, acted effectively as a diffusion barrier which inhibited the outward diffusion of titanium species. After 240 h exposure, an outer-layer of TiO_2 with 190 μm thickness formed for the uncoated titanium whilst the thickness of the outer TiO_2 layer developed on the uncoated Ti–6Al–4V alloy was 70 μm. However, the thickness of the TiO_2 outer-layer which formed on the Nb-coated Ti and Ti–6Al–4V alloy after 240 h exposure was only ~ 16 μm. Secondly, the

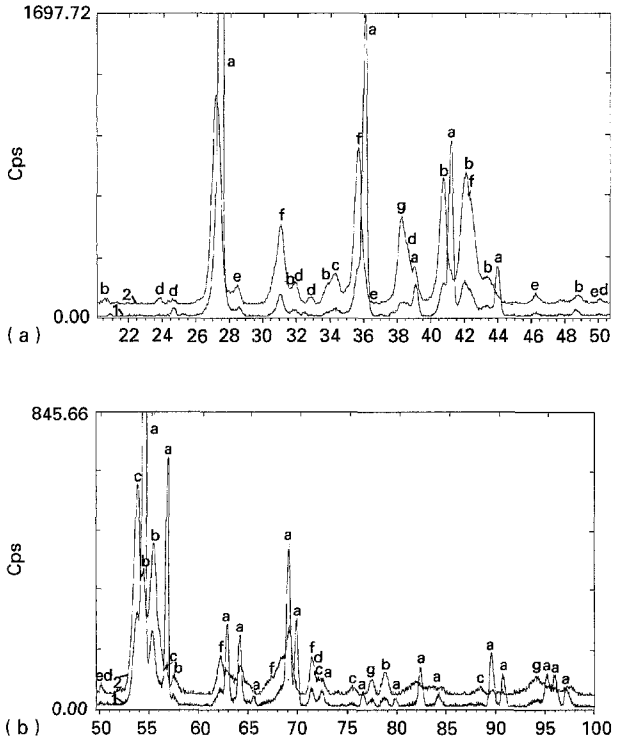

Figure 9 XRD profiles of Nb-coated Ti–6Al–4V alloy after 168 h exposure in an $H_2/H_2O/H_2S$ ($pS_2 \sim 10^{-1}$ Pa and $pO_2 \sim 10^{-18}$ Pa) environment at 750 °C. (a) Theta = 20–50 degree; (b) Theta = 50–100 degree.

formation of the $Nb_{1-x}S$ scale on the surface of the Nb coating at the initial stages of exposure further enhanced its corrosion resistance. The expected low sulphidation rate of pure bulk niobium observed previously ($K_p \sim 10^{-13}\,g^2\,cm^{-4}\,s^{-1}$ [16]) in this low oxygen and high sulphur potential environment was not fully realized in these Nb-coated materials. If the niobium coating used here had sulphidized at the reported rate with $K_p \sim 10^{-13}\,g^2\,cm^{-4}\,s^{-1}$ [16], then 6 μm thickness of the Nb coating could have lasted about 10^4 h. However, in this study, after 168 h exposure, there was little evidence of the existence of Nb coating on either Ti or Ti–6Al–4V alloy. It is believed that the laminated structure of $Nb_{1-x}S$ [30], which developed at the early stages of exposure, intercalated with Ti species which migrated from the substrate and therefore, enhanced the niobium diffusion in the $Nb_{1-x}S$ scale and the Nb coating was rapidly consumed. Consequently the expected long life of the Nb coating was substantially reduced. A similar hypothesis was postulated concerning the development of MoS_2 in Co–Mo alloys containing up to 40 wt % Mo exposed to a sulphur vapour at temperatures between 550–900 °C [24].

The mechanisms for the sulphidation/oxidation of uncoated Ti and Ti–6Al–4V alloy at 750 °C in $H_2/H_2O/H_2S$ atmosphere have been elucidated in another paper [4]. It was established that the outer-layer of TiO_2 formed by the outward diffusion of titanium species, whilst the mid-layer of TiO_2 developed by the ingress of oxygen species. Simultaneously, the TiS_2 inner-layer on Ti, and Al_2S_3 and TiS_2 layer on the Ti–6Al–4V alloy were considered to form together with the oxide layers. After the oxide/sulphide scale developed, a concentration gradient of the reactants (O, S, Ti, Al, V) was established. At the oxide/sulphide interface, Al_2S_3 became unstable and decomposed to release S and Al which produced a reservoir of aluminium. The outward migration of aluminium from this reservoir resulted in the precipitation of the thermodynamically favoured product Al_2O_3 in the external portion of the outer-layer. In the meantime the liberated sulphur species diffused through the sulphide layer towards the substrate and reacted with titanium and aluminium to form TiS_2 and Al_2S_3. It is believed that the same process was responsible for the precipitation of TiO_2 in titanium.

However, the degradation processes for the Nb-coated Ti and Ti–6Al–4V alloy followed a complex pattern. Figs 4 and 5 indicate that a $Nb_{1-x}S$ layer was formed as the Nb-coated samples were exposed to the high sulphur potential environment. With increasing exposure time, Ti species migrated outwards through the Nb-coating and the $Nb_{1-x}S$ scale to form an outer-layer of TiO_2 above the $Nb_{1-x}S$ layer. Also the sulphur species diffused inwards, reached the coating/substrate interface and produced TiS_2 for Ti, as shown in Figs 4, 6 and 7, and a mixture of Al_2S_3 and TiS_2 for the Ti–6Al–4V alloy (Figs 8 and 9). The formation of the $Nb_{1-x}S$ layer separated the Nb coating from the TiO_2 outer-layer and resulted in a decrease in niobium activity at the $TiO_2/Nb_{1-x}S$ interface. Further instability occurred due to the decrease in pS_2 at this interface. Consequently the $Nb_{1-x}S$ formed at the interface decomposed and released niobium and sulphur species. The niobium species so released encountered the incoming oxygen species from the environment diffusing through the TiO_2 outer-layer and developed NbO_2 and Nb_2O_5 at the $TiO_2/Nb_{1-x}S$ interface, as revealed in Figs 6 and 8. A series of XRD experiments on the exposed Nb-coated specimens for various exposure periods confirmed that niobium oxides were hardly detected during short exposure periods (e.g. up to 24 h) although the outermost TiO_2 layer did not grow quickly. With increasing exposure time (e.g. 168 h, the intensities of niobium oxides in XRD profiles became evident, as shown in Figs 7 and 9. At the same time, the incoming oxygen species also reacted with the titanium species from the substrate to form TiO_2. There is a suggestion that Nb_2O_5 and TiO_2 form a solid solution [31, 32]. Also, the freed sulphur species generated from the dissociation of $Nb_{1-x}S$ diffused inwards towards the sulphide/substrate interface to generate TiS_2 for Ti and $Al_2S_3 + TiS_2$ for the Ti–6Al–4V alloy respectively and thereby thickened the sulphide layers. However, due to the formation of TiS_2 or Al_2S_3/TiS_2, the Ti or Al activities at the sulphide/coating interface were reduced and therefore the sulphides probably became unstable and dissociated to produce free sulphur, titanium and aluminium species. The released sulphur species migrated through the sulphide layers and produced TiS_2 or Al_2S_3 at the sulphide/substrate interface. It appears that the titanium and aluminium species reacted with the incoming oxygen species to form the corresponding oxides, as shown in Figs 6 and

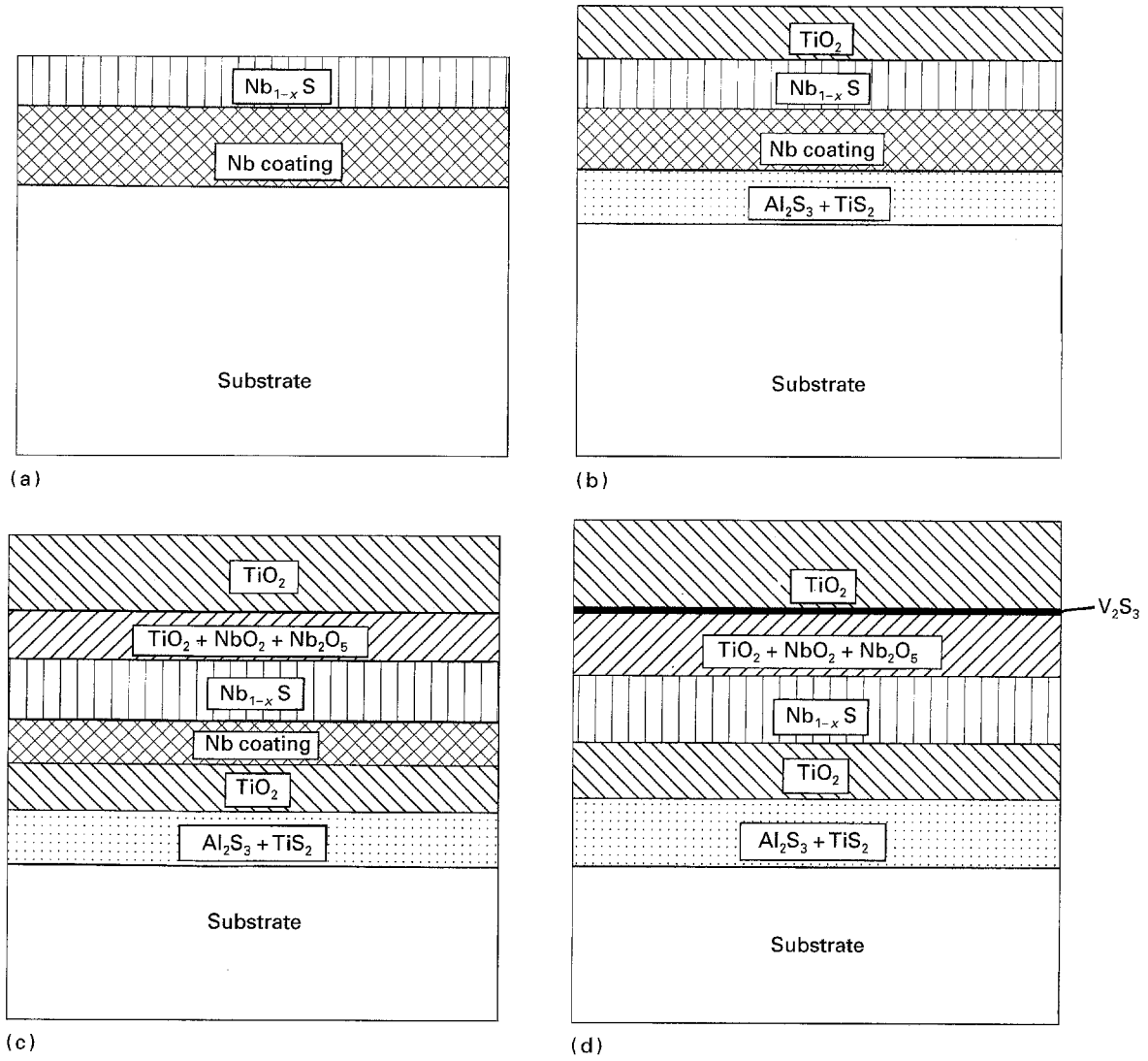

Figure 10 The schematic model describing the degradation processes of the Nb-coated Ti–6Al–4V alloy. (a) Formation of $Nb_{1-x}S$ layers. (b) Formation of TiO_2 and $Al_2S_3 + TiS_2$ layers. (c) Partial dissociation of $Nb_{1-x}S$ and $Al_2S_3 + TiS_2$ layers and formation of $TiO_2 + NbO_2 + Nb_2O_5$ and inner TiO_2 layers. (d) Final state.

8. The amount of Al_2O_3 was too small to be detected by XRD.

In the case of the Ti–6Al–4V alloy, a thin vanadium sulphide (possibly V_2S_3) layer was also observed at the interface of the outer TiO_2 layer and $NbO_2 + Nb_2O_5 + TiO_2$ mixed layer. From thermodynamic considerations, the low dissociation partial pressure of V_2S_3 ($\sim 10^{-25}$ Pa) would make it possible to form V_2S_3 at this interface by the outward diffusion of vanadium from the substrate. It is believed that the formation of the vanadium sulphide layer, acting as a diffusion barrier, further increased the corrosion resistance of the Nb-coated Ti–6Al–4V alloy. The suggested degradation processes for the Nb-coated Ti–6Al–4V alloy are schematically illustrated in Fig. 10. A similar corrosion model is suggested to be operative for the Nb coated Ti except that Al_2S_3 and V_2S_3 would not form.

5. Conclusions

1. In an $H_2/H_2O/H_2S$ test environment ($pS_2 \sim 10^{-1}$ Pa and $pO_2 \sim 10^{-18}$ Pa) at 750 °C the corrosion behaviour of titanium showed a linear rate law whilst that of Ti–6Al–4V alloy followed linear-parabolic kinetics.

2. The Nb coating produced by the arc deposition process increased the corrosion resistance of Ti and Ti–6Al–4V alloy, both showing parabolic rate laws with a slight departure after long-term exposure.

3. The corrosion products generated on pure titanium were characterized by a double layered oxide scale of TiO_2 beneath which a TiS_2 layer was observed. For the Ti–6Al–4V alloy, α-Al_2O_3 was precipitated in the external portion of the outer-layer of TiO_2; whilst a layer of Al_2S_3, TiS_2 and vanadium sulphide (possibly V_2S_3) was found underlying the inner TiO_2 layer.

4. A scale following the sequence $TiO_2/TiO_2 + NbO_2 + Nb_2O_5/Nb_{1-x}S/TiO_2/TiS_2/$(substrate) was observed on Nb-coated Ti, whilst a scale represented by the sequence $TiO_2/V_2S_3/TiO_2 + NbO_2 + Nb_2O_5/Nb_{1-x}S/TiO_2/Al_2S_3 + TiS_2/$(substrate) characterized the corrosion products formed on the Nb-coated Ti–6Al–4V alloy.

5. The Nb coating used acted as an effective diffusion barrier, blocking the outward diffusion of titanium species and inward migration of sulphur and oxygen species. The formation of $Nb_{1-x}S$ scale further enhanced the corrosion resistance of the Nb-coated samples. However the enhancement of corrosion resistance by Nb coating decreased with increasing exposure time probably due to the intercalation of $Nb_{1-x}S$ with Ti species.

Acknowledgements

Grateful acknowledgement is given to the financial funding of Dr H. L. Du, as a Research Fellow, at the University of Northumbria at Newcastle, and Dr D. B. Lewis, as a Senior Research Fellow at Sheffield Hallam University, by the UK's Science and Engineering Research Council's Rolling Grant in Surface Engineering.

References

1. P. K. DATTA, K. N. STRAFFORD and A. L. DOWSON in Proceedings of Second Irish Conference on Durability and Fracture, 1984, edited by J. Bolton and S. Hampshire.
2. *Idem.*, International Symposium on Light Metals, India.
3. A. L. DOWSON, PhD thesis, Newcastle Polytechnic, 1988.
4. H. L. DU, P. K. DATTA, B. LEWIS, and J. S. BURNELL-GRAY, *Oxid. Met.* in press.
5. *Idem.*, *Corr. Sci.* **36** (1994) 631.
6. I. A. MENZIES and K. N. STRAFFORD, *Ibid.* **7** (1967) 23.
7. *Idem.*, *J. Less-Common Metals* **12** (1967) 85.
8. A. M. CHAZE and C. CODDET, *Oxid. Met.* **21** (1984) 205.
9. A. RAHMEL and P. J. SPENSER, *Ibid.* **35** (1991) 53.
10. K. L. LUTHRA, *Ibid.* **36** (1991) 475.
11. P. KOFSTAD, "High Temperature Corrosion" (Elsevier Applied Science Publishers 1988).
12. S. BECKER, A. RAHMEL, M. SCHORR and M. SCHUTZE, *Oxid. Met.* **38** (1992) 425.
13. P. K. DATTA, internal report, University of Northumbria at Newcastle, 1988.
14. K. N. STRAFFORD and P. K. DATTA, *Mater. Sci. Technol.* **5** (1989) 765.
15. K. N. STRAFFORD, P. K. DATTA and J. S. GRAY, in Surface Engineering Practice, International Conference on Advances in Coatings and Surface Treatments, Newcastle upon Tyne, 1988, edited by K. N. Strafford, P. K. Datta and J. S. Gray, p. 397.
16. D. JENKINSON, PhD Thesis, University of Northumbria at Newcastle, 1983.
17. W. Y. CHAN, PhD Thesis, University of Northumbria at Newcastle, 1985.
18. H. L. DU, PhD Thesis, University of Northumbria at Newcastle, 1991.
19. GE WANG, R. CARTER and D. L. DOUGLASS, *Oxide. Met.* **32** (1989) 273.
20. B. GLEESON, D. L. DOUGLASS and F. GESMUNDO, *Ibid.* **31** (1989) 209.
21. M. F. CHEN, D. L. DOUGLASS and F. GESMUNDO, *Ibid.* **31** (1989) 273.
22. R. V. CARTER, D. L. DOUGLASS and F. GESMUNDO, *Ibid.* **31** (1989) 341.
23. M. F. CHEN and D. L. DOUGLASS, *Ibid.* **32** (1989) 185
24. B. GLEESON, D. L. DOUGLASS and F. GESMUNDO, *Ibid.* **33** (1990) 425.
25. H. L. DU, L. P. WARD, J. S. GRAY, P. K. DATTA, B. LEWIS and A. MATTHEWS, in Mat-Tec 91, International Conference Proceedings, Paris, 1991, p. 159.
26. L. P. WARD, H. L. DU, J.S. GRAY, P.K. DATTA, B. LEWIS and A. MATTHEWS, in Mat-Tec 91, International Conference Proceedings, Paris, 1991, p. 165.
27. P. K. DATTA, K. N. STRAFFORD, H. L. DU, B. LEWIS and J. S. GRAY, in Proceedings of First International Conference, on Heat Resistant Materials, Fontana, Wisconsin, 1991, edited by K. Natesan and D. J. Tillack, p. 323.
28. H. L. DU, P. K. DATTA, J. S. GRAY and K. N. STRAFFORD, *Oxide. Met.* **39** (1993) 107.
29. H. L. DU, P. K. DATTA, J. S. BURNELL-GRAY and K. N. STRAFFORD, *Corr. Sci.* **36** (1994) 99.
30. F. KADIJK and F. JELLINEK, *J. Less-Common Met.* **19** (1969) 421.
31. P. KOFSTAD, *Ibid.* **12** (1967) 449.
32. Y. S. CHEN and C. J. ROSA, *Oxid. Mat.* **14** (1980) 147.

Received 3 February
and accepted 16 November 1994